DESY 95-011
February 1995

HERA+LC Based γp Collider: Luminosity and Physics

Z. Z. Aydin

II. Institut für Theoretische Physik, Universität Hamburg

A. T. Alan, S. Atağ, O. Çakir, A. Çelikel, A. K. Çiftçi, A. Kandemir, S. Sultansoy, Ş. Türköz, Ö. Yavaş, M. Yilmaz, A. U. Yilmazer

Ankara University, Faculty of Sciences, Physics Department, Turkey

ISSN 0418-9833

DESY 95-014 ISSN 0418-9833

HERA+LC Based γp Collider: Luminosity and Physics

Z.Z. Aydın*
II. Institut für Theoretische Physik der Universität Hamburg

A.T. Alan†, S. Atağ, O. Çakır, A. Çelikel, A.K. Çiftçi, A. Kandemir
S. Sultansoy‡, Ş. Türköz, Ö. Yavaş, M. Yılmaz§ and A.U. Yılmazer
Ankara University, Faculty of Sciences, Physics Department, Ankara, Turkey

ABSTRACT

We discuss the possibility of constructing a Linac-Ring type ep collider and a γp collider based on it at DESY, namely the HERA+LC proposal. Using the parameters of the proton ring of HERA and those of the proposed linear e^+e^- collider (LC), we expect a luminosity of $L_{\gamma p} = (1-2) \times 10^{31} cm^{-2} s^{-1}$ due to reasonable improvement of the proton beam. In a γp collider, high energy γ beam is produced by the Compton backscattering of laser photons off electron beam from linear accelerator. In the case of opposite choice of laser photon and electron beam helicities, the luminosity of γp collisions still exceeds $10^{31} cm^{-2} s^{-1}$ up to a distance of $12m$ between the conversion region and the collision point. We examine the physics research program for the HERA+LC γp collider proposal. Search for the supersymmetric partners, leptoquark production as well as heavy quark investigation are considered in detail. The capacity of HERA+LC surpasses that of HERA and is comparable with LC. Polarization facilities of the gamma and proton beams, and the clearer background compared to the hadron colliders are stated as additional advantages of the proposed γp collider.

*Alexander von Humboldt fellow. On leave of absence from Ankara University
†İnönü University, Physics Department, Malatya, Turkey
‡Permanent address: Institute of Physics, Academy of Sciences, Baku, Azerbaijan
§Gazi University, Physics Department, Ankara, Turkey

I. INTRODUCTION

The electron-proton collisions have played an important role in our understanding of the substructure of matter. For example, starting with the celebrated experiments at SLAC in the 1970's the quark-parton model has been inspired from the deep inelastic ep scattering. These fixed target experiments have at most reached the center-of-mass energies of the order of $\sqrt{s} \leq 30$ GeV. For higher energies, standard ep colliders have been proposed in 1980's. i.e., HERA at DESY and LHC+LEP at CERN. The ep collider HERA, with two independent rings, has now been in operation for two years with a center-of-mass energy $\sqrt{s} = 297$ GeV (26.7 GeV for electrons and 820 GeV for protons). This corresponds to $\sqrt{s} \sim 100$ GeV at the quark constituent level and shows that the standard ep colliders HERA and LHC+LEP are far from reaching the TeV energy scale at a subprocess level. However, physicists believe that new physics beyond the standard model (SM) should exist at the TeV scale. The reason for this belief is that although the SM has been succesful in the description of the elementary particles and their interactions up to the scale of 100 GeV, it does not explain a number of principal problems, i.e. the existence of the three fermion families, the large difference between fermion masses ($m_{\nu_e} < 10$ eV, $m_t > 130$ GeV), fine tuning between Fermi and Planck scales etc. Various approaches towards the new physics at the TeV scale such as extended electroweak symmetry, technicolor, supersymmetry and preonic composite model have been proposed.

In order to reach TeV energies at the constituent level, new accelerator developments are necessary. Now it is widely believed that because of large energy losses due to synchrotron radiation the electrons in ep machines should be accelerated linearly. In this connection, two types of Linac-Ring ep machines are proposed: one of them is combining the existing e^+e^- linear collider proposals with the large hadron machines, another type is adding a special electron linac to the proton storage ring.

For the first time, linac-ring type ep colliders were considered by Csonka and Rees [1] in connection with SLAC electron accelerator. The possibility of colliding the electron beam from VLEPP with UNK proton beam [2] was the main reason for dislocation of VLEPP from Novosibirsk to Protvino. Then, Grosse-Wiessmann proposed to construct special electron linacs in addition to LHC and SSC [3]. Some combinations of large hadron machines and e^+e^- colliders were considered in Ref. [4] in order to obtain TeV energies in ep collision. A very attractive feature of these new type ep machines is the possibility of constructing a γp collider practically with the same c.m. energy (in the TeV range) and with the same high luminosity [4–6]. The research program of a γp collider based on the UNK+VLEPP proposal was considered in Refs. [7–13]. Recently different physics phenomena which can be investigated at γp colliders have been considered in a number of papers [14–21]. It seems that these machines open new possibilities for investigation of the Standard Model and beyond it.

In this paper, we concentrate ourselves on the γp collider based on the proposed linac-ring type ep machine, HERA+LC. We estimate the main parameters of this collider and discuss the new physics that we can investigate with this machine, such as searches for the supersymmetric particles, excited quarks and leptoquarks, and the heavy quark production.

II. MACHINE

A. Linac-Ring type ep Colliders

Two versions of ep collisions are possible for linac-ring type machines: in the proton ring and on the extracted proton beam. In the former case proton bunches with maximal number of protons will be used repeatedly, the advantage of the second version is maximal compression of proton bunches in collision region. We have already discussed these two versions in Ref. [4–6] and come to a conclusion that the second version might be promising only for UNK+VLEPP and LHC+TESLA proposals. Here we concentrate ourselves on the version of collisions in the proton ring.

Most important limitation on the luminosity in this case follows from the condition of the stability of the proton bunch after the collision with the electron bunch:

$$\frac{n_e}{s_e} = 7 \cdot 10^{18} \frac{E_p}{TeV} \frac{cm}{\beta_p} \Delta Q_p \frac{1}{cm^2} \tag{1}$$

where n_e is the number of electrons in a bunch. The transverse area, s_e, is equal to $4\pi\sigma_x\sigma_y$, where σ_x and σ_y are horizontal and vertical sizes of electron bunch at the collision point. E_p, β_p and ΔQ_p are the energy, the amplitude function at the intersection point and the tune shift of the proton beam, respectively. The restriction of $\Delta Q_p \leq 0.003$ takes place for hadron colliders. In our case admitted values for ΔQ_p may be larger because each proton bunch makes many revolutions between two sequential collisions with electron bunches. This point should be investigated but here we will use the conservative restriction of $\Delta Q_p \leq 0.003$. Therefore, the luminosity of ep collisions is given by

$$\mathcal{L}_{ep} = n_e f_e \frac{n_p}{s_{eff}}. \tag{2}$$

where s_{eff} is the larger of s_p and s_e obtained from Eq.(1). The luminosity is restricted from above, and its maximum value at $n_p = 10^{12}$ is equal to

$$\mathcal{L}_{ep}^{\max} = 2.1 \cdot 10^{28} f_e \frac{E_p}{TeV} \frac{cm}{\beta_p} \frac{1}{cm^2} \tag{3}$$

where $f_e = f_{rep} n_b$ is the frequency of electron bunches.

Numerical values of $\mathcal{L}_{ep}$ for different proposals computed with the above considerations are given in Ref. [6]. The main parameters of the proposed linac-ring type ep machine HERA+LC are as follows

	$\sqrt{s}$	s_e^{min}	$\mathcal{L}_{ep}^{max}$	δ
$HERA+LC$	$1.28TeV$	$12 \times 10^{-6} cm^2$	$1.5 \times 10^{31} cm^{-2} s^{-1}$	4×10^{-4}

Now let us come to energy losses of electrons during collisions with a proton bunch. Electrons oscillate around the beam axis because of the electromagnetic field of the proton bunch. This causes to the bremsstrahlung of electrons. The fractional energy loss is given by [3]

$$\delta = \frac{\Delta E_e}{E_e} = \left(\frac{n_p}{10^{12}}\right)^2 \frac{cm}{\sigma_z} \frac{(\mu m)^2}{\sigma_x \sigma_y} \frac{E_e}{TeV} \tag{4}$$

which yields the value 4×10^{-4} for HERA+LC.

B. High Energy γ Beam

The idea [22] of obtaining high energy photon beams by Compton backscattering of laser light off a beam of high energy electrons was already proposed for γe and $\gamma\gamma$ colliders [23–28]. The same method can be used for constructing γp colliders if linear e^+e^- machines or special e-linacs are to be built up near the large proton rings, see Fig. 1. The essence of this method is as follows: A beam of laser photons ($w_0 \sim 1$eV) with high intensity, about 10^{20} photons per pulse, is Compton backscattered off high energy electrons from a linear accelerator and turns into hard photons with a conversion coefficient close to unity. Both the scattered electrons and the backscattered photons follow the incident electron beam direction within a few microradian (of course, the scattered electrons can be deflected away from the interaction point by a transverse magnetic field in order to reduce backgrounds). The energy of converted photons, E_γ, is restricted by the condition $y_{max} = 0.83$ (where $y = E_\gamma / E_e$) in order to get rid off background effects, in particular, e^+e^- pair production in the collision of a laser photon with a high energy photon in the conversion region.

The details of the Compton kinematics and calculations of the cross section can be found in Refs. [25,26,28]. The differential cross section is

$$\frac{1}{\sigma}\frac{d\sigma}{dy} \equiv f_\gamma(y) = \frac{1}{\sigma}\frac{2\pi\alpha^2}{\zeta m_e^2}\left[1 - y + \frac{1}{1-y} - \frac{4y}{\zeta(1-y)} + \frac{4y^2}{\zeta^2(1-y)^2} - \lambda_e\lambda_\gamma \frac{y(2-y)}{(1-y)}\left(\frac{2y}{\zeta(1-y)} - 1\right)\right] \tag{5}$$

where $\zeta = 4E_e\omega_0/m_e^2$ and the total Compton cross section σ is

$$\sigma = \sigma^0 + \lambda_e\lambda_\gamma\sigma^1 \tag{6}$$

$$\sigma^0 = \frac{\pi\alpha^2}{\zeta m_e^2}\left[(2 - \frac{8}{\zeta} - \frac{16}{\zeta^2})ln(\zeta+1) + 1 + \frac{16}{\zeta} - \frac{1}{(\zeta+1)^2}\right] \tag{7}$$

$$\sigma^1 = \frac{\pi\alpha^2}{\zeta m_e^2}\left[(2 + \frac{4}{\zeta})ln(\zeta+1) - 5 + \frac{2}{(\zeta+1)} - \frac{1}{(\zeta+1)^2}\right] \tag{8}$$

The energy spectrum of the backscattered photons, $f_\gamma(y)$, is plotted in Fig. 2 for unpolarized beams and for the values of $\zeta = 1.5, \zeta = 3.0$ and $\zeta = 4.8$. The value $y_{max} = 0.83$ corresponds to $\zeta = 4.83$. For comparison we also plot

here the spectrum of the bremsstrahlung photons, which up to now were used for the study of γp interactions in ep collisions. We have to emphasize that the spectral distribution and mean helicity of the photon beam substantially change by polarizing both the electron beam and the laser light: if the electrons and laser have the same (opposite) polarization the resulting spectrum is relatively flat (more monocromatic peaking at very high energy). Polarizing the electrons or laser also results in polarized high energy photons.

More details on high energy γ beam, as well as requirements on lasers can be found in Refs. [25–28].

As we have already mentioned, two versions of ep and γp collisions (on the extracted proton beam and in the proton ring) are possible. According to Ref. [4], the second is more promising. The nonexistence of the non-stability problem of proton bunches after the collision for γp regime, in contrary to the ep regime, is a very important feature. In this case the expression for the luminosity of a γp collider has the following form (factor 2 reflects that $s_\gamma \ll s_p$):

$$\mathcal{L}_{\gamma p} = 2(n_\gamma n_p/s_p)\nu_\gamma, \tag{9}$$

where ν_γ is the collision frequency, $n_\gamma = n_e$ (we suggest that the conversion coefficient is equal to 1) and n_p are numbers of particles in corresponding bunches. The transverse area, s_p, is given as $4\pi\epsilon\beta/\gamma$, where ϵ is the normalized emittance of the proton beam, β is the amplitude function at the intersecting point, and γ is the Lorentz factor of the proton. Note that in the case of a multi-bunch structure of electron linac pulses $\nu_\gamma = f_{rep} n_b$, where n_b is the number of bunches per pulse-train.

The main parameters of the proton and electron beams for HERA+LC are $E_p = 0.82$ TeV, $E_e = 0.5$ TeV, $n_p = 10^{12}$, $n_e = 2.1 \times 10^{10}$, $s_p = 1.4 \times 10^{-5} cm^2$, $f_{rep} = 50Hz$, $n_b = 172$. Using them we immediately get the luminosity for HERA+LC as $\mathcal{L}_{\gamma p} = 2.5 \times 10^{31}\ cm^{-2}s^{-1}$.In fact,at DESY presently two different alternatives for the next linear e^+e^- collider (LC) are being investigated: (i) DESY/THD (S-band collider design) and (ii) TESLA (Superconducting collider design). Both are multi-national collaborations. Although we use the parameters of the S-band choice,the TESLA alternative will also give essentially the same (actually two times higher) luminosity for the HERA+TESLA γp collider.

There are a number of design problems associated with realizing γp colliders. The main part of them is similar to the known design problems of γe colliders (see Ref. [27]). Technical solutions of these problems depend on parameters of electron and proton beams, used in each proposed γp machine. In our recent work [29], the effect of distance and the helicities as well as design problems for different γp colliders have been discussed. Here, we give three figures from the above mentioned reference concerning the HERA+LC proposal. In Fig.3 dependence of luminosity on the distance between the conversion region and the collision point is plotted for different choices of laser photons and electron beam helicities. The advantage of choosing opposite helicities is obvious. In this case $L_{\gamma p}$ still exceeds the value of $10^{31} cm^{-2}s^{-1}$ up to distances of $z = 12m$. Fig.4 shows luminosity distributions depending on γp invariant mass $W_{\gamma p} = 2\sqrt{E_\gamma E_p}$ at $z = 6m$. Again the advantage of opposite helicities of laser photons and electron beam is obvious. In Fig.5 the above mentioned distributions are given for the $\lambda_e = 1, \lambda_0 = -1$ choice at three different values of distance between the conversion region and the collision point. This figure reflects that better monochromatization for interacting photons can be achieved by increasing the distance.

III. PHYSICS

A. Search for SUSY

Among various possibilities to go beyond the SM the supersymmetry (SUSY) idea seems to be a strong candidate to open the new horizon for the TeV scale physics [30]. The search for supersymmetry is therefore one of the major tasks of the present and future particle accelerators. The minimal particle content of any supersymmetric extension of the standard model leads necessarily to the doubling of the usual particle spectrum. It is highly believed that superpartners of the known particles should have masses below 1 TeV in order not to loose the good features of the SUSY. In this section we will present the recent results of the analysis for the supersymmetric particle production at the HERA+LC γp collider.

The literature on the survey of the supersymmertic particle production mechanisms is very rich and the results of the experiments in hadron-hadron colliders, ep-machines and e^+e^--accelerators indicate that the masses of squarks and gluinos are $m_{\tilde{q},\tilde{g}} \geq 100GeV$ and those of the sleptons $m_{\tilde{l}} \geq 45GeV$ [31]. Consequently higher energy scales should be probed and it is desirable to reach the TeV scale at a constituent level. Therefore it might be sensible to say that HERA, LEP, Fermilab and LHC should be sufficient to check the idea of low energy SUSY, namely the scale below 1 TeV, however experiments at all possible types of colliding beams would be inevitable to explore the new physics at the TeV scale.

The production and the detection of supersymmetric particles in hadron-hadron collisions, lepton-hadron collisions and e^+e^- annihilations have been extensively studied but any experimental evidence is still lacking.Accurate computations of cross-sections, branching ratios and their detailed background analysis within the minimal supersymmetric standard model framework are available. The experimental challenge is intensively continuing . On the other hand, the high energy photon-proton scattering mentioned in the previous section allows new sparticle production mechanisms in a very interesting mass range. Also, expected clearer backgrounds compared to the hadron colliders raise the question of the physics potential of a γp-collider in search for supersymmetry. In the following sub-sections we will present the cross-sections for various SUSY production processes and indicate the discovery mass limits for squarks, gluinos, charginos and neutralinos. Our calculations have been done within the minimal supersymmmetric extension of the standard model (MSSM) which includes soft breaking terms [30].Here we have only taken into account the direct interaction of the photon with partons in the proton. The resolved contributions to the associated productions of SUSY particles and heavy quark pair production are relatively small, around 10% [33] which do not affect our rough estimates for the discovery mass limits of new particles very much.For heavy quark pair production, $x_{min} \geq 0.1$,but for the $\bar{c}c$ and $\bar{b}b$ production the main contribution will come from extremely small x-region and then one has to worry about the hadronic component of the photon.

1. Associated squark-wino production

The differential cross section of the subprocesses $\gamma q \rightarrow \tilde{w}\tilde{q}$ has the following form:

$$\begin{aligned}\frac{d\hat{\sigma}}{d\hat{t}} = \frac{\pi\alpha^2}{\hat{s}^2\sin^2\theta_W}\{&Q_q^2\frac{(\tilde{M}_w^2-\hat{t})}{\hat{s}} + Q_w^2\frac{\hat{s}(\tilde{M}_w^2-\hat{t})+2\tilde{M}_w^2(\tilde{M}_d^2-\hat{t})}{(\hat{t}-\tilde{M}_w^2)^2}\\ &+ Q_s^2\frac{(\hat{s}+\hat{t}-\tilde{M}_d^2)(\hat{s}+\hat{t}-\tilde{M}_w^2-2\tilde{M}_d^2)}{(\tilde{M}_w^2-\hat{s}-\hat{t})^2}\\ &+ 2Q_wQ_q\frac{(\tilde{M}_d^2-\hat{t})(\hat{s}+\tilde{M}_w^2-\tilde{M}_d^2)+\hat{s}\tilde{M}_w^2}{\hat{s}(\hat{t}-\tilde{M}_w^2)}\\ &+ Q_qQ_s\frac{\hat{s}(\hat{s}+\hat{t})+2\hat{t}(\tilde{M}_w^2-\tilde{M}_d^2)-\tilde{M}_d^2(2\tilde{M}_w^2-2\tilde{M}_d^2+3\hat{s})}{\hat{s}(\tilde{M}_w^2-\hat{s}-\hat{t})}\\ &+ Q_wQ_s\frac{\hat{s}(\tilde{M}_w^2-\hat{t})-\hat{t}^2+3\hat{t}(\tilde{M}_w^2+\tilde{M}_d^2)+2\tilde{M}_d^2(\hat{s}-\tilde{M}_d^2)-3\tilde{M}_d^2\tilde{M}_w^2}{(\hat{t}-\tilde{M}_w^2)(\tilde{M}_w^2-\hat{s}-\hat{t})}\}\end{aligned} \tag{10}$$

One can easily perform the integration over $d\hat{t}$ and get the total cross section $\hat{\sigma}$ for the subprocess $\gamma q \rightarrow \tilde{w}\tilde{q}$. In order to obtain the total cross section for the process $\gamma p \rightarrow \tilde{w}\tilde{q}X$ one should integrate $\hat{\sigma}$ over the quark and photon distributions:

$$\sigma = \int_{\frac{(\tilde{M}_w+\tilde{M}_d)^2}{s}}^{0.83} d\tau \int_{\frac{\tau}{0.83}}^{1} dx \frac{1}{x}[f_\gamma(\frac{\tau}{x})f_q(x)]\hat{\sigma}(\tilde{M}_w, \tilde{M}_d, \hat{s}) \tag{11}$$

where $f_q(x)$ is the distribution of quarks inside the proton [32], and $f_\gamma(y)$ is the energy spectrum of the high energy real photons given in Eq.(5). The details may be found in [16]. If the observation limit is taken to be 100 events per running year one can easily extract the upper mass limits for the supersymmetric particle observations. The corresponding values are

$$\begin{aligned}\tilde{m}_w = \tilde{m}_d &= 0.2TeV\\ \tilde{m}_d = 0.4TeV \quad &\text{for} \quad \tilde{m}_w = 0.1TeV\\ \tilde{m}_w = 0.25TeV \quad &\text{for} \quad \tilde{m}_d = 0.1TeV\end{aligned}$$

In Fig. 6 the dependence of the total cross section on the masses of SUSY particles is depicted.

2. Associated gluino-squark and neutralino squark production

In this case the subprocesses to be considered are $\gamma q \rightarrow \tilde{q}\tilde{g}$ and $\gamma q \rightarrow \tilde{q}\tilde{\gamma}$ (or $\tilde{q}\tilde{z}$). After straightforward manipulations the differential cross section for the subprocess takes the form

$$\frac{d\hat{\sigma}}{d\hat{t}} = C\frac{1}{\hat{s}^2}\left\{\frac{\tilde{M}^2-\hat{t}}{\hat{s}} + \frac{(\hat{t}+\hat{s})(\hat{t}+\hat{s}-\tilde{M}^2-3\tilde{M}_q^2)+\tilde{M}_q^2(\tilde{M}^2+2\tilde{M}_q^2)}{(\hat{s}+\hat{t}-\tilde{M}^2)^2}\right.$$
$$\left. - \frac{2(\hat{t}-\tilde{M}_q^2)(\tilde{M}^2-\tilde{M}_q^2)+\hat{s}(\hat{s}+\hat{t}-3\tilde{M}_q^2)}{\hat{s}(\hat{s}+\hat{t}-\tilde{M}^2)}\right\} \tag{12}$$

$$C = \frac{C_{L,R}^2}{32\pi}$$

The factors $C_{L,R}$ are given as

$$C_L = C_R = N_c e Q_q g_s \qquad \text{for} \quad \tilde{g} \quad \text{and} \quad \tilde{q}_{L,R}$$

$$C_L = \sqrt{2}(eQ_q)^2 = -C_R \qquad \text{for} \quad \tilde{\gamma} \quad \text{and} \quad \tilde{q}_{L,R}$$

$$C_L = -\frac{\sqrt{2}geQ_q}{cos\theta_W}(T_{3q} - Q_q sin^2\theta_W) \qquad \text{for} \quad \tilde{z} \quad \text{and} \quad \tilde{q}_L \tag{13}$$

$$C_R = -\frac{\sqrt{2}geQ_q^2}{cos\theta_W} sin^2\theta_W \qquad \text{for} \quad \tilde{z} \quad \text{and} \quad \tilde{q}_R$$

where θ_W is the weak mixing angle, Q_q is the electric charge of the quark and N_c is the color factor, see Ref. [19]. The discovery mass limits for squarks, gluinos and neutralinos are as follows :

$$\tilde{m}_g = 0.32TeV \quad \text{for} \quad \tilde{m}_q = 0.1TeV$$
$$\tilde{m}_q = 0.2TeV \quad \text{for} \quad \tilde{m}_g = 0.1TeV$$
$$\tilde{m}_q = \tilde{m}_g = 0.18TeV$$

Also for a luminosity ten times larger we find :

$$\tilde{m}_q = 0.17TeV \quad \text{for} \quad \tilde{m}_\gamma = 0.05TeV$$
$$\tilde{m}_q = 0.15TeV \quad \text{for} \quad \tilde{m}_z = 0.1TeV$$
$$\tilde{m}_z = \tilde{m}_q = 0.13TeV$$

Again Fig. 7 and Fig. 8 show the total cross sections versus sparticle masses.

3. Pair production of squarks

The differential cross section of the subprocess $\gamma g \rightarrow \tilde{q}\tilde{q}^*$ under consideration can be calculated as

$$\frac{d\hat{\sigma}}{d\hat{t}} = \frac{e^2e_{\tilde{q}}^2g_s^2}{\pi\hat{s}^2}\left[1 + \frac{m_{\tilde{q}}^2(3m_{\tilde{q}}^2-\hat{s}-\hat{t})}{2(\hat{s}+\hat{t}-m_{\tilde{q}}^2)^2} + \frac{(3m_{\tilde{q}}^2-\hat{s}+\hat{t})}{4(m_{\tilde{q}}^2-\hat{t})^2}\right.$$
$$\left. + \frac{(5m_{\tilde{q}}^2+2\hat{s}-\hat{t})}{4(\hat{s}+\hat{t}-m_{\tilde{q}}^2)} + \frac{(\hat{s}-2m_{\tilde{q}}^2)(\hat{s}-4m_{\tilde{q}}^2)}{4(m_{\tilde{q}}^2-\hat{t})(\hat{s}+\hat{t}-m_{\tilde{q}}^2)}\right] \tag{14}$$

After performing the integration over $\hat{t}$ one can easily obtain the total cross section for the subprocess $\gamma g \rightarrow \tilde{q}\tilde{q}^*$ as follows :

$$\hat{\sigma}(\hat{s}, m_{\tilde{q}}) = \frac{\pi\alpha e_{\tilde{q}}^2\alpha_s}{2\hat{s}}\left[2\beta(2-\beta^2) - (1-\beta^4)ln\frac{1+\beta}{1-\beta}\right] \tag{15}$$

where $\beta = (1-4m_{\tilde{q}}^2/s)^{1/2}$. The above expression in Eq.(15) is a cross section for left- squarks or right-squarks only and a color factor of $C = 1/2$ is already included. In order to obtain the total cross section for the process $\gamma p \rightarrow \tilde{q}\tilde{q}^* X$ one can integrate $\hat{\sigma}$ over the gluon and photon distributions:

$$\sigma = \int_{4m_{\tilde{q}}^2/s}^{0.83} d\tau \int_{\tau/0.83}^{1} dx \frac{1}{x} f_\gamma(\frac{\tau}{x}) f_g(x) \hat{\sigma}(s, m_{\tilde{q}}) \tag{16}$$

where $f_g(x)$ is the distribution of gluons inside the proton [32]:

$$f_g(x) = \frac{1}{x}\left[(2.62 + 9.17x)(1-x)^{5.90}\right] \tag{17}$$

and f_γ is given in Eq.(5).

Actually the production of squark pairs in collisions via the quasi-real photon gluon fusion were studied in Ref. [33]. However the Weizsacker-Williams approximation has been used for the quasi-real photon distribution, and since the WW-spectrum is much softer than the real γ spectrum the mass limits for the squarks in our case turn out to be much higher than the conventional ep-colliders. The discovery mass limit for the squarks at HERA+LC is 200 GeV. The production cross section as a function of the squark mass is given in Fig. 9. Ref. [18] gives the calculational details.

4. Signature and Conclusion

The possible decay modes of squarks, gluinos, neutralinos and charginos depend on the mass spectrum and on the parameters which are responsible for the supersymmetry breaking. Due to the recent calculations on the mass relations and constraints from the top quark mass the ordering for the masses of the SUSY particles, starting with the lightest one, can be taken as $\tilde{\gamma}, \tilde{z}, \tilde{w}, \tilde{h}, \tilde{l}, \tilde{q}$, and $\tilde{g}$. Then the squark will mainly decay into a quark and a photino. There also exist additional decay modes for the squark into a wino or a zino with less branching ratios. The gluino will decay into a squark and antiquark. The dominant decay mode of zino will be the decay into a neutralino, quark and antiquark. Usually the photino and sneutrino are taken as the lightest SUSY particles and will not be observed like neutrinos. Therefore the signature for the processes under consideration might be as follows:

$$\begin{array}{rcl}
\tilde{w}^+\tilde{d} \rightarrow jet + l^+ + p_T^{miss} & \text{or} & 3jets + p_T^{miss} \\
\tilde{g}\tilde{q} \rightarrow 3jets + p_T^{miss} & or & multijets + p_T^{miss} \\
\tilde{q}\tilde{\gamma} \rightarrow jet + p_T^{miss} & or & 3jets + p_T^{miss} \\
\tilde{q}\tilde{z} \rightarrow jet + p_T^{miss} & or & 3jets + p_T^{miss} \\
\tilde{q}\tilde{q}^* \rightarrow 2jets + p_T^{miss} & or & multijets + l(s) + p_T^{miss}
\end{array}$$

To conclude, our analysis shows that the future γp-colliders will have equally well capacities in the investigations of the supersymmetric particles. We observe that the range of squark masses that can be explored at the HERA+LC γp-machine (200 GeV - 400 GeV) are much higher than the corresponding values at the HERA ep-collider (20 GeV - 80 GeV).

B. Excited Quark Production

In composite models of leptons and quarks excited particles naturally occur. The single resonance production of excited quarks is a simple and direct way of searching for the signals of compositeness in γp collisions. The cross section $\hat{\sigma}$ for the subprocess $\gamma q \rightarrow q^*$ is given by the well known Breit-Wigner formula

$$\hat{\sigma} = \frac{(4\pi)^2}{M_{q^*}^2} \frac{(2J+1)}{2\times 2} \frac{\Gamma(q^* \rightarrow q\gamma)}{M_{q^*}}, \tag{18}$$

where J is the excited quark spin and Γ is the width of the excited quark decay along the channel $q^* \rightarrow q\gamma$. Further integration over the photon spectrum and quark distributions in the proton should be performed:

$$\sigma = \int_{\tau_{min}}^{0.83} d\tau \int_{\tau/0.83}^{1} \frac{dx}{x} f_\gamma\left(\frac{\tau}{x}\right) f_q(x) \hat{\sigma}(\tau s), \tag{19}$$

where

$$\tau_{min} = \frac{(M_{q^*})^2}{s}, \qquad \hat{s} = \tau s,$$

and f_γ is the energy spectrum of the backscattered photons from electrons, Eq.(5). $f_q(x)$ is the sum of valence and sea quark distribution functions with momentum fraction x inside the proton, taken from Eichten *et al.*, set 1 in Ref. [32]. In numerical calculation we consider the excited u^* quark production for the proposed γp machine. The total cross sections are plotted against excited quark masses in Fig. 10 for $\sqrt{s} = 1.28$ TeV. Taking 100 events/year as a reasonable discovery limit for the excited quark searches we obtain an upper limit for the excited quark mass of about 1 TeV.

The main decay mode of excited quark will be $q^* \to qg$ and manifest itself as an invariant mass peak in two-jet events with a large transverse momentum.

C. Leptoquark Production

For scalar and vector leptoquark interactions with fermions we write the following most general lagrangian [34] which is invariant under $SU(3)_C \times SU(2)_W \times U(1)_Y$:

$$L = L_S + L_V \tag{20}$$

with

$$\begin{aligned} L_S = {} & g_{1L}\bar{q}_L^c i\tau_2\, \ell_L S_1 + g_{1R}(\bar{u}_R^c e_R + \bar{d}_R^c \nu_R) S_1' + \tilde{g}_{1R}\bar{d}_R^c e_R \tilde{S}_1 \\ & + \tilde{g}_{1R}'\bar{u}_R^c \nu_R \tilde{S}_1' + g_{3L}\bar{q}_L^c i\tau_2 \vec{\tau}\ell_L \vec{S}_3 \\ & + h_{2L}\bar{u}_R \ell_L R_2 + h_{2R}\bar{q}_L i\tau_2 e_R R_2' + \tilde{h}_{2L}\bar{d}_R \ell_L \tilde{R}_2 + \tilde{h}_{2R}\bar{q}_L i\tau_2 \nu_R \tilde{R}_2' + h.c., \end{aligned} \tag{21}$$

$$\begin{aligned} L_V = {} & (g_{2L}\bar{d}_R^c \gamma^\mu \ell_L + g_{2R}\bar{q}_L^c \gamma^\mu e_R) V_{2\mu} \\ & + \tilde{g}_{2L}\bar{u}_R^c \gamma^\mu \ell_L \tilde{V}_{2\mu} + g_{2R}'\bar{q}_L^c \gamma^\mu \nu_R V_{2\mu}' \\ & + (h_{1L}\bar{q}_L \gamma^\mu \ell_L + h_{1R}\bar{d}_R \gamma^\mu e_R + h_{1R}\bar{u}_R \gamma^\mu \nu_R) U_{1\mu} \\ & + \tilde{h}_{1R}\bar{u}_R \gamma^\mu e_R \tilde{U}_{1\mu} + \tilde{h}_{1R}'\bar{d}_R \gamma^\mu \nu_R \tilde{U}_{1\mu}' + h_{3L}\bar{q}_L \vec{\tau}\gamma^\mu \ell_L \vec{U}_{3\mu} + h.c., \end{aligned} \tag{22}$$

where L_S and L_V denote the scalar and vector leptoquark lagrangians, respectively. q_L and ℓ_L are the $SU(2)_W$ left handed quark and lepton doublets, and $\psi^c = C\bar{\psi}^T$ is the charge conjugated fermion field. Leptoquarks U_1, $\tilde{U}_1$ $\tilde{U}_1'$ and S_1, S_1', $\tilde{S}_1$, $\tilde{S}_1'$ are $SU(2)_W$ singlets, V_2, V_2', $\tilde{V}_2$ and R_2, R_2', $\tilde{R}_2$, $\tilde{R}_2'$ are $SU(2)_W$ doublets and U_3 and S_3 are $SU(2)_W$ triplets. The subscripts L and R of the coupling constants refer to lepton chirality. Each type of leptoquarks is a color triplet. The lagrangian (20) differs from the one of Ref. [34] by the terms having right handed neutrino. In our opinion,the inclusion of these terms is quite reasonable because of the lepton-quark symmetry. There are constraints imposed on leptoquark masses and coupling constants from low energy experiments [35–38]. The lower bounds on the masses of leptoquarks involving electrons arising from low energy leptonic π decays and atomic parity violations lie above 600 or 700 GeV when the coupling is of electromagnetic strength. Much weaker constraints on μq type leptoquarks occur. From here on the conventional parametrization $g_i^2 = 4\pi\alpha_{em}k_i$ will be used to scale coupling contants to electromagnetic coupling, where $g_{2L}...h_{3L}$ are replaced by g_i.

1. Single Production of Leptoquarks

It is known that (eu) and (ed) type leptoquarks can be produced singly at the ep collider HERA via electron-quark fusion process. In hadron colliders single leptoquarks of (eq), (μq) and (τq) type are produced in association with leptons through quark-gluon collision. In addition, single leptoquarks of any type can also be produced in γp colliders by exploiting photon-quark collisions. Single leptoquarks can be produced through the subprocess $\gamma q \to V(S)$ where q refers to u and d quarks, and V(S) to any type of vector(scalar) leptoquarks. The possible types of leptoquarks which can be produced in γp collision are shown in Table I. The Feynman amplitude consists of t, u and s channels which correspond to lepton, leptoquark and quark exchanges, respectively. Using the interaction lagrangian (20) it is straightforward to obtain the cross sections [15] in terms of Mandelstam variables for the subprocess $\gamma q \to Sl$.

$$\frac{d\hat{\sigma}}{d\hat{t}} = \frac{|M_{fi}|^2}{16\pi(\hat{s} - m_q^2)^2} \tag{23}$$

$$
\begin{aligned}
|M_{fi}|^2 = (4\pi\alpha_{em})^2 k \Bigg\{ & \frac{Q_S^2 M_S^2}{(\hat{t}-M_S^2)^2}\left[M_\ell M_q + M_\ell^2 + M_q^2 - \hat{t}\right] \\
& + \frac{Q_\ell Q_S}{(M_q^2+M_S^2-\hat{s}-\hat{t})(\hat{t}-M_S^2)}\left[M_\ell^2(\hat{s}+\hat{t}-M_\ell^2) - M_q^2(\hat{s}-M_\ell^2-M_S^2)\right. \\
& \left. - M_S^2(M_\ell^2+M_q^2-\hat{t})\right] + \frac{Q_S Q_q}{(\hat{s}-M_q^2)(\hat{t}-M_S^2)}\left[M_\ell^2(\hat{s}+\hat{t}-M_\ell^2)\right. \\
& \left. + M_q^2(\hat{s}-M_\ell^2-M_S^2) + M_S^2(M_\ell^2+M_q^2-\hat{t})\right] \\
& + \frac{Q_\ell^2}{(M_q^2+M_S^2-\hat{s}-\hat{t})^2}\left[4M_q^2M_\ell^2 - 2M_\ell^2(\hat{s}+\hat{t}-M_\ell^2) - \tfrac{1}{2}(\hat{s}+\hat{t}-M_\ell^2)\,(\hat{s}-M_\ell^2-M_S^2)\right. \\
& \left. + \tfrac{1}{2}(M_\ell^2+M_q^2-\hat{t})(M_S^2-M_q^2-M_\ell^2) + M_q^2(\hat{s}-M_\ell^2-M_S^2)\right] \\
& + \frac{Q_\ell Q_q}{(\hat{s}-M_q^2)(M_q^2+M_S^2-\hat{s}-\hat{t})}\left[8M_\ell^2M_q^2 + 8M_\ell M_q(M_\ell^2+M_q^2+\tfrac{M_S^2}{2})\right. \\
& + 3M_q^2(\hat{s}-M_\ell^2-M_S^2) - 3M_\ell^2(\hat{s}+\hat{t}-M_\ell^2) - (M_\ell^2+M_q^2-\hat{t})(M_\ell^2+M_q^2) \\
& \left. - (\hat{s}+\hat{t}-M_\ell^2)\,(\hat{s}-M_\ell^2-M_S^2)\right] + \frac{Q_q^2}{(\hat{s}-M_q^2)^2}\left[4M_q^2M_\ell^2 + 2M_q^2(\hat{s}-M_\ell^2-M_S^2)\right. \\
& \left. - M_\ell^2(\hat{s}+\hat{t}-M_\ell^2) + \tfrac{1}{2}(M_\ell^2+M_q^2-\hat{t})(M_S^2-M_\ell^2-M_q^2)\right. \\
& \left. - \tfrac{1}{2}(\hat{s}+\hat{t}-M_\ell^2)\,(\hat{s}-M_\ell^2-M_S^2)\right]\Bigg\}
\end{aligned}
\tag{24}
$$

where $\hat{s} = (p_\gamma + p_q)^2$, $\hat{t} = (p_\ell - p_q)^2$, and p_γ, p_q, p_ℓ and M_S represent photon, quark, lepton momenta and scalar leptoquark mass, respectively.

Then following the similar steps of the previous section we calculate total cross sections for the reaction $\gamma p \to S\ell X$ considering the photon spectrum and quark distribution in the proton.

In numerical calculations we consider the subprocess $\gamma u \to Se^-, S\mu^-, S\tau^-$. The total cross sections against scalar leptoquark masses are plotted in Fig. 11 for HERA+LC.

TABLE I. Types and charges (Q) of scalar and vector leptoquarks which can be produced in γp collision. LH and RH denote left handed and right handed.

Process	Q	Type (Scalar)	Type (Vector)
$\gamma u \to Ve^-(Se^-)$	5/3	$R_2(LH)$	$U_1(RH), U_3(LH)$
$\gamma u \to Ve^+(Se^+)$	-1/3	$S_1(LH), S_1'(RH), S_3(LH)$	$V_2(RH), \tilde{V}_2(LH)$
$\gamma d \to Ve^-(Se^-)$	2/3	$R_2'(RH), \tilde{R}_2(LH)$	$U_1(LH), U_1(RH), U_3(LH)$
$\gamma d \to Ve^+(Se^+)$	-4/3	$\tilde{S}_1(RH), S_3(LH)$	$V_2(LH), V_2(RH)$
$\gamma u \to V\nu(S\nu)$	2/3	$R_2(LH), \tilde{R}_2'(RH)$	$U_1(LH), U_3(LH), U_1(RH)$
$\gamma u \to V\bar{\nu}(S\bar{\nu})$	2/3	$S_3(LH), \tilde{S}_1'(RH)$	$\tilde{V}_2(LH), V_2'(RH)$
$\gamma d \to V\nu(S\nu)$	-1/3	$\tilde{R}_2(LH), \tilde{R}_2'(RH)$	$U_3(LH), \tilde{U}_1'(RH)$
$\gamma d \to V\bar{\nu}(S\bar{\nu})$	-1/3	$S_1(LH), S_3(LH), S_1'(RH)$	$V_2(LH), V_2'(RH)$

Since the leptoquark couples to $q\ell$ and $q\nu$, one anticipates the following signals for single leptoquark production: (a) $j + 2\ell$, (b) $j + \ell + p_T^{miss}$ or (c) $j + p_T^{miss}$. The background comes from the standard model processes: $\gamma q \to Zq$ for the case (a) and (c), and $\gamma q \to Wq$ for the case (b). In order to eliminate these effects we make the requirement that the leptoquark signal has a sharp invariant mass peak in $M_{j\ell}$ at M_V which is absent in the standard model processes. Furthermore, W and Z signals include mass peaks in $M_{\ell p_T^{miss}}$ and $M_{\ell^+\ell^-}$ at M_W and M_Z which are not present in the leptoquark production. The signal (a) is the most striking one for the existence of leptoquarks. Thus, when compared with hadron colliders γp machines probably have a clear background for the leptoquark production. This allows us to demand 100 or less events per year for the discovery limit for the leptoquark searches. Using the γp luminosities for HERA+LC and cross sections from Fig. 11 we find the upper mass limits for the scalar leptoquarks of the (eu), (μu), (τu) kinds. We consider the scaling parameter $k = 1$ for the coupling constants and the resultant upper mass limits are given as

0.60	TeV	for	(eu)	kind
0.50	TeV	for	(μu)	kind
0.45	TeV	for	(τu)	kind

2. Pair Production of Leptoquarks

The leptoquark pair can be produced via the subprocess $\gamma g \to \bar{V}V(\bar{S}S)$ in γp collision. The Feynman diagrams contributing to this process include t and u channels which correspond to the leptoquark exchange, and the quartic vertex $\gamma g\bar{V}V(\gamma g\bar{S}S)$. In the case of scalar leptoquarks the total cross section for the subprocess is found to be

$$\hat{\sigma}(\hat{s}) = \frac{N_c \pi \alpha Q_S^2 \alpha_s}{\hat{s}} \left[2\beta(2-\beta) + (1-\beta^4) \ln \frac{1-\beta}{1+\beta} \right], \tag{25}$$

and in the case of vector leptoquarks it is given by

$$\hat{\sigma}(\hat{s}) = \frac{N_c \pi \alpha \alpha_s Q_V^2}{(1-\beta^2)\hat{s}} \left[2\beta(22 - 9\beta^2 + 3\beta^4) + 3(1 - \beta^2 - \beta^4 + \beta^6) \ln\left(\frac{1-\beta}{1+\beta}\right) \right], \tag{26}$$

with

$$\beta = \sqrt{1 - \frac{4M_{LQ}^2}{\hat{s}}},$$

where $\hat{s}$, α_s and $N_c = 1/2$ are the Mandelstam variable, strong coupling constant and color factor from the average over the incoherent sum, respectively. M_{LQ} denotes the vector or scalar leptoquark mass. Following the similar steps of the previous section, we integrate Eq.(25) or Eq.(26) over gluon and photon distributions in order to obtain the total cross section for the process $\gamma p \to \bar{V}VX(\bar{S}SX)$:

$$\sigma = \int_{\tau_{min}}^{0.83} d\tau \int_{\tau/0.83}^{1} \frac{dx}{x} f_\gamma\left(\frac{\tau}{x}\right) f_g(x) \hat{\sigma}(\tau s), \tag{27}$$

with

$$\tau_{min} = \frac{4M_{LQ}^2}{s},$$

where $f_g(x)$ is given in Eq.(17) The strong coupling constant α_s has been evaluated at $Q^2 = \hat{s}/2$ with the parametrization of Eichten *et al.*, in Ref. [32]. Fig. 12 shows the behaviour of the cross section as a function of the scalar leptoquark masses . One should note that the coupling constant is model independent in the case of pair production.

The pair production of leptoquarks gives the signals (a) $2j + \ell\bar{\ell}$ (b) $2j + \ell\nu$ (c) $2j + \nu\bar{\nu}$. The recognition of (a) is the easiest one since the signal for pair production of leptoquark shows a pair of sharp peaks with the same invariant mass $M_{j\ell}$. Moreover, the jets in the leptoquark decay will be widely seperated. Thus, the pair production of leptoquarks is, in principle, free of background coming from the standard model processes. Taking 100 events per year as discovery limit, the upper observable mass limit of the scalar leptoquarks with charge Q=5/3 turns out to be 0.3 TeV.

D. Heavy Quark Production

In this section we analyse the goals of the HERA+LC γp collider in heavy quark searches. It seems that the t quark will be discovered in the near future at FNAL with an improved luminosity, because there are strong arguments in favor that $m_t \leq 250$ GeV. According to D0 Collaboration experimental lower limit for t-quark mass is 130 GeV and CDF Collaboration reports evidence for the existence of the t-quark with mass 174 ∓ 10 GeV [39]. For this reason we estimate the number of $\bar{t}t$ pairs which will be produced at HERA+LC for different values of m_t (150, 200 and 250 GeV). Then we obtain the discovery limits for heavy quarks, a fourth SM family of t' and b' quarks or isosinglet D quarks predicted by the E_6 model [40–42]. Finally, we give short remarks on the possibility of investigating extremely small x_g via process $\gamma p \to \bar{c}cX$ or $\bar{b}bX$.

The quark-antiquark pairs will be produced through the subprocess $\gamma g \to \bar{q}q$. The Feynman amplitudes consist of two well-known diagrams and it is easy to obtain the differential cross section

$$\frac{d\hat{\sigma}}{d\hat{t}} = \frac{|M|^2}{16\pi\hat{s}^2} \tag{28}$$

$$|M|^2 = 32\pi^2\alpha_{em}\alpha_s Q^2 C\left[\frac{4m^2\hat{s}}{(\hat{t}-m^2)(\hat{u}-m^2)} + \frac{\hat{u}-m^2}{(\hat{t}-m^2)} + \frac{\hat{t}-m^2}{(\hat{u}-m^2)} - \frac{4m^4\hat{s}^2}{(\hat{t}-m^2)^2(u-m^2)^2}\right] \tag{29}$$

where $\hat{s} = (p_\gamma + p_g)^2, \hat{t} = (p_\gamma - p_q)^2, \hat{u} = (p_q - p_g)^2$ are Lorentz invariant Mandelstam variables; p_γ, p_g, p_q and m denote photon, gluon, quark momenta and quark mass, respectively. α_{em} is the fine structure constant and α_s is the strong coupling constant. Q is the charge of quarks, and the color factor C is 1/2.

In order to find the cross section for the subprocess $\gamma g \to \bar{q}q$, the integration over $\hat{t}$ can be carried out analytically. We get

$$\hat{\sigma} = \frac{\pi\alpha_{em}\alpha_s Q^2}{\hat{s}(1+\beta^2)}\left[2\beta(\beta^4 - \beta^2 - 2) + (\beta^6 + \beta^4 - 3\beta^2 - 3)\ln\left(\frac{1-\beta}{1+\beta}\right)\right] \tag{30}$$

where $\beta = \sqrt{1 - 4m^2/s}$. Further integration over the gluon distribution in the proton and the energy spectrum of the photon should be performed to obtain the cross section for the quark pair production through the process $\gamma p \to \bar{q}qX$:

$$\sigma = \int_{\tau_{min}}^{0.83} d\tau \int_{\tau/0.83}^{1} \frac{dx}{x} f_\gamma\left(\frac{\tau}{x}\right) f_g(x)\hat{\sigma}(\tau s) \tag{31}$$

where $\tau_{min} = 4m^2/s$ and $\hat{s} = \tau s$.

The gluon distribution function in the proton at $x > 0.01$ has been chosen as in Eq.(17). At $x < 0.01$ different parametrization were proposed. We use two possibilities taken from [32]

$$f_g(x) = \frac{1}{x}(0.444x^{-1/2} - 1.886) \tag{32}$$

$$f_g(x) = 25.56x^{-1/2}. \tag{33}$$

The total cross sections versus the quark mass are plotted in Fig. 13 for HERA+LC γp collider in the case of $Q = 2/3$. For heavy quarks with charge $Q = -1/3$ the cross section decreases by a factor 1/4.

The numbers of $\bar{t}t$ pairs which will be produced at the γp collider under consideration are given in Table II for three different values of m_t.

In the last columns of Table II we give the observable upper masses for new quarks. Here we take 100 events per year as the discovery limits for new quarks at γp colliders. This value is quite reasonable due to clearer situation concerning the background as compared to $\bar{p}p$ and pp colliders. In the Table II, t' and b' denote the fourth fermion family quarks, D denotes the weak isosinglet heavy quark with Q=-1/3 predicted by the E_6 model.

Signatures for new quark production will depend on their masses and mixings. Note that the lightest of t' and b' will decay only due to mixing with the first three family quarks. Let us suppose that the mixing between fourth and third family quarks dominates. Therefore, if $m_{t'} > m_{b'}$ (or $m_{b'} > m_{t'}$) the dominant mode for b'(or t') decay will be

$b' \to t + W$(or $t' \to b + W$). Then, if $m_{t'} > m_{b'} + m_W$, the dominant decay mode will be $t' \to b' + W$. As a result the signature for the t' and b' search is similar (may be a little more complicated to those for t-quark).

A different situation takes place for D-quark decays because flavor changing neutral currents appear. Indeed, the D-quark will decay due to mixings with usual down-type quarks. Let us suppose that the interfamily mixing dominates and we restrict ourselves to the consideration of the first E_6 family quarks:

$$\begin{pmatrix} u^\theta \\ d^\phi \end{pmatrix}_L \quad , \quad u_R, \quad d_R, \quad D_L^\phi, \quad D_R \tag{34}$$

where $d^\phi = d\cos\phi + D\sin\phi$, $D^\phi = -d\sin\phi + D\cos\phi$. Here we have supposed that usual CKM mixings lie in the up-quark sector, the subscript θ reflects this fact.

Mixing between left-handed components of d and D leads to a modification of the Lagrangian. The interaction Lagrangian responsible for D-quark decays has the form:

$$\begin{aligned} \mathcal{L} = & \frac{\sqrt{4\pi\alpha_{em}}}{2\sqrt{2}\sin\theta_W}\left[\bar{u}^\theta\gamma_\alpha(1-\gamma_5)d\cos\phi + \bar{u}^\theta\gamma_\alpha(1-\gamma_5)D\sin\phi\right]W_\alpha \\ & - \frac{\sqrt{4\pi\alpha_{em}}}{4\sin\theta_W}\left[\frac{\sin\phi\cos\phi}{\cos\theta_W}\bar{d}\gamma_\alpha(1-\gamma_5)D\right]Z_\alpha + h.c. \end{aligned} \tag{35}$$

In Eq.(35) θ_W denotes the Weinberg angle, $\sin^2\theta_W \sim 0.23$. In order to keep Cabibbo universality, ϕ must be restricted by $\sin^2\phi \leq 0.01$. In accordance with Eq.(35), for the partial decay widths of the D-quark one has

$$\Gamma(D \to u^\theta W) = \frac{\alpha_{em}}{16} f_W m_D \sin^2\phi \tag{36}$$

$$\Gamma(D \to dZ) = \frac{\alpha_{em}}{32(1-\sin^2\theta_W)} f_Z m_D \sin^2\phi\cos^2\phi \tag{37}$$

where $f_V = (1-\epsilon_V)^2(1+\epsilon_V)/\epsilon_V$, $\epsilon_V = m_V^2/m_D^2$ $(V = W, Z)$. Notice that the experimental lower limit for the D-quark mass is the same as for the t-quark, namely $m_D > 130GeV$. Therefore we can neglect the difference in the W and Z mode phase factors because $m_Z - m_W \sim 10GeV$. As a result, one has the branching ratios $\mathrm{BR}(D \to uW) \sim 0.6$ and $\mathrm{BR}(D \to dZ) \sim 0.4$. Therefore the essential part of the D-decays will be induced by flavor changing neutral currents. In particular, $D \to d\ell^+\ell^-(\ell = e, \mu, \tau)$ decay channels occur with probability more than 1%.

As mentioned above, γp colliders will give the opportunity to investigate gluon distributions at extremely small x_g by means of the processes $\gamma p \to \bar{c}cX$ and $\gamma p \to \bar{b}bX$. In Fig. 14 we represent the $\bar{c}c$ pair production differential cross-section, $d\sigma/dx_g$, for the HERA+LC proposal. As one can see from this figure, parametrizations (32) and (33) lead to drastically different behaviours at small x_g. Note that these parametrizations are not valid at $x_g < 10^{-4}$ however we represent this region for illustration. Then, the main part of the $\bar{c}c$ pairs will be produced at extremely small $x_g \simeq 10^{-5}$. Therefore, the proposed γp machines will give the opportunity to investigate gluon distributions up to $x_g \simeq 10^{-5}$, where the phenomenon of inverse evolution of parton distributions [43] will manifest itself. Detailed investigation of these aspects as well as the role of the hadronic component of the photon will be considered elsewhere.

TABLE II. Number of $\bar{t}t$ pair production per year and discovery limits for new quarks.

Machines	$N_{\bar{t}t}(10^3)$				
	150 GeV	200 GeV	250 GeV	$m_{t'}(TeV)$	$m_{b',D}(TeV)$
HERA+LC	1.7	0.4	0.1	0.25	0.20

ACKNOWLEDGEMENTS: One of the authors (Z.Z.A.) would like to thank Professor G.Kramer for the hospitality at the II. Institut für Theoretische Physik der Universität Hamburg,for his critical reading of the manuscript and valuable suggestions.

[1] P.L.Csonka and J.Rees, Nucl. Instr. & Meth. **96** (1971) 146.
[2] S.I.Alekhin et al., IHEP preprint 87-48, Serpukhov (1987).
[3] P.Grosse-Wiesmann, Nucl. Instr. & Meth. A **274** (1989) 21.
[4] S.F.Sultansoy, ICTP preprint IC/89/409, Trieste (1989).
[5] Z.Z.Aydin, V.A.Maniyev and S.F.Sultansoy, Particle World. **4** (1994) 22.
[6] Z.Z.Aydin, A.K.Ciftci and S.F.Sultansoy, Nucl. Instr. & Meth. A **351** (1994) 261.
[7] S.I.Alekhin et al., IHEP preprint 88-94, Serpukhov (1988).
[8] S.I.Alekhin et al., Proc. of the Int. Symposium "Hadron Interactions-Theory and Phenomenology", (Prague, 1988) p.360.
[9] S.I.Alekhin et al., Proc. of XI Seminar "Problems on High Energy Physics and Field Theory", (Moscow, Nauka, 1989) p.328.
[10] G.Jikia, Nucl.Phys. B **333** (1990) 317.
[11] S.I.Alekhin et al., Int. J. of Mod. Phys. A **6** (1991) 23.
[12] E.Boos et al., DESY preprint 91-114, Hamburg (1991).
[13] E.Boos et al., Proc. 26^{th} Moriond Conf. on Electroweak Interactions and Unified Theories, (Moriond, France, 1991) p.501.
[14] W.Buchmüller and Z.Fodor, Phys. Lett. B **316** (1993) 510.
[15] S.Atag, A.Çelikel and S. Sultansoy, Phys. Lett. B **326** (1994) 185.
[16] A.T.Alan, Z.Z.Aydin and S.Sultansoy, Phys. Lett. B **327** (1994) 70.
[17] S. Atag and O. Çakır, Phys. Rev. D **49** (1994) 5769
[18] A.T.Alan, A.Kandemir and A.U.Yilmazer, Ankara University preprint AU/94-07(HEP) (1994).
[19] A.T.Alan, S.Atag and Z.Z.Aydin, J. Phys. G **20** (1994) 1399.
[20] O. Çakır and S. Atağ, Ankara University preprint AU/94-10(HEP) (1994).
[21] O. Çakır, S. Sultansoy and M. Yılmaz, Ankara University preprint AU/94-11 (HEP) 1994.
[22] R.N.Milburn, Phys. Rev. Lett. **10** (1963) 75.
[23] I.F.Ginzburg et al., Piz'ma ZhETF **34** (1981) 514.
[24] I.F.Ginzburg et al., Yad. Fiz. **38** (1983) 372.
[25] I.F.Ginzburg et al., Nucl. Inst. & Meth. **205** (1983) 47.
[26] I.F.Ginzburg et al., Nucl. Inst. & Meth. **219** (1984) 5.
[27] V.I.Telnov, Nucl. Inst. & Meth. A **294** (1990) 72.
[28] D.L.Borden, D.A.Bauer and D.O.Caldwell, SLAC preprint SLAC-PUB-5715, Stanford (1992).
[29] A.K.Ciftci, S.Sultansoy, S.Turkoz and O.Yavas, Ankara University Preprint AU/95-01(HEP) (1995).
[30] H.E.Haber and G.L.Kane, Phys.Rep.C117,75(1986)
H.P.Nilles,Phys.Rep.C110,1, (1984)
C.H.Llewellyn-Smith, Phys.Rep. C105, 53 (1884)
[31] Review of Particle Properties, Phys. Rev. D **50** (1994) 1227.
[32] E.Eichten *et al.*, Rev. Mod. Phys. **56** (1984) 579.
[33] M.Drees and K.Grassie, Z. Phys. C **28** (1985) 451.
[34] W. Buchmüller, R. Rückl, and D. Wyler, Phys. Lett. B **191**, 442 (1987).
[35] W. Buchmüller and D. Wyler, Phys. Lett. B **177**, 377 (1986).
[36] O. Shanker, Nucl. Phys. B **206**, 49 (1982).
[37] M. Leurer, Phys. Rev. D **49**, 333 (1994)
[38] S. Davidson, D. Bailey and B.A. Campbell Z. Phys. C **61**, 613 (1994)
[39] S. Abachi *et al.* (D0 Collaboration), Phys. Rev. Lett. **72** (1994) 2138; F. Abe *et al.* (CDF Collobaration), FNAL preprint FERMILAB-PUB-94/116-E (1994).
[40] F. Gürsey, P. Ramond and P. Sikivie, Phys. Lett. B **60** (1976) 177.
[41] F. Gürsey and M. Serdaroğlu, Lett. Nuovo Cimento **21** (1978) 28 ; Il Nuovo Cimento **65** A (1981) 337.
[42] J.L. Hewet and T.G. Rizzo, Phys. Rep. **183** (1989) 193.
[43] V.L. Gribov *et al.*, Phys. Rep. C **100** (1981) 1.

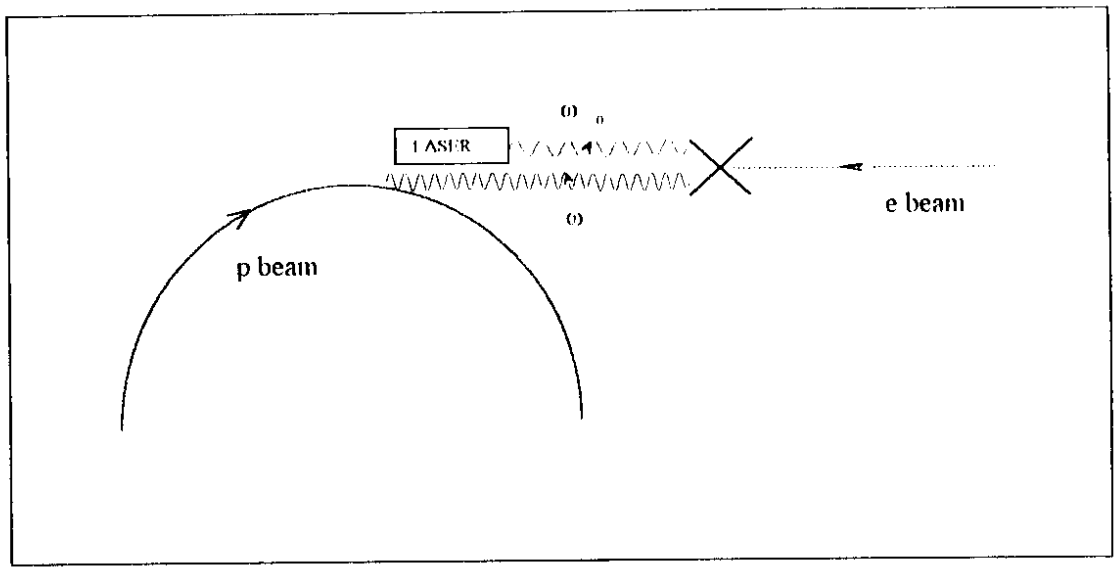

FIG. 1. Schematic view of the proposed machine.

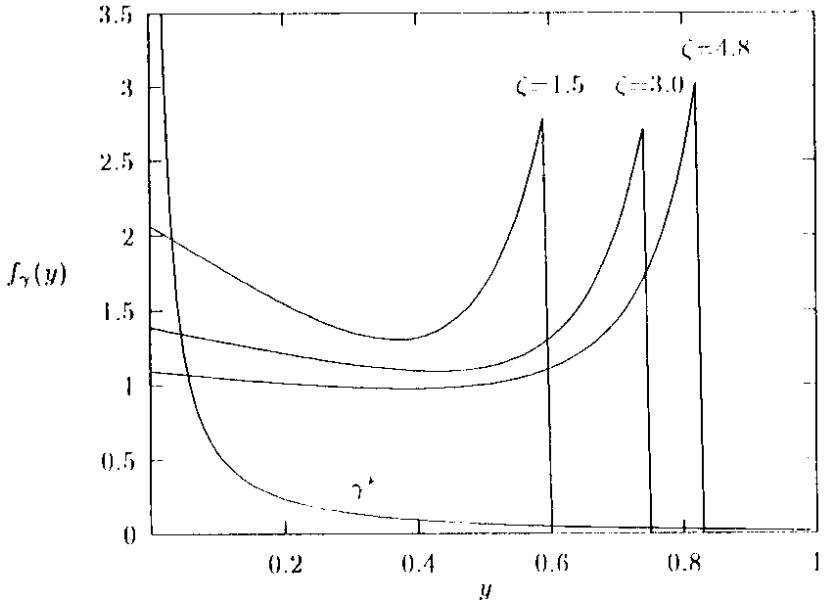

FIG. 2. Energy spectrum of backscattered photons for unpolarized beams. The curve γ^* shows the spectrum of bremsstrahlung photons.

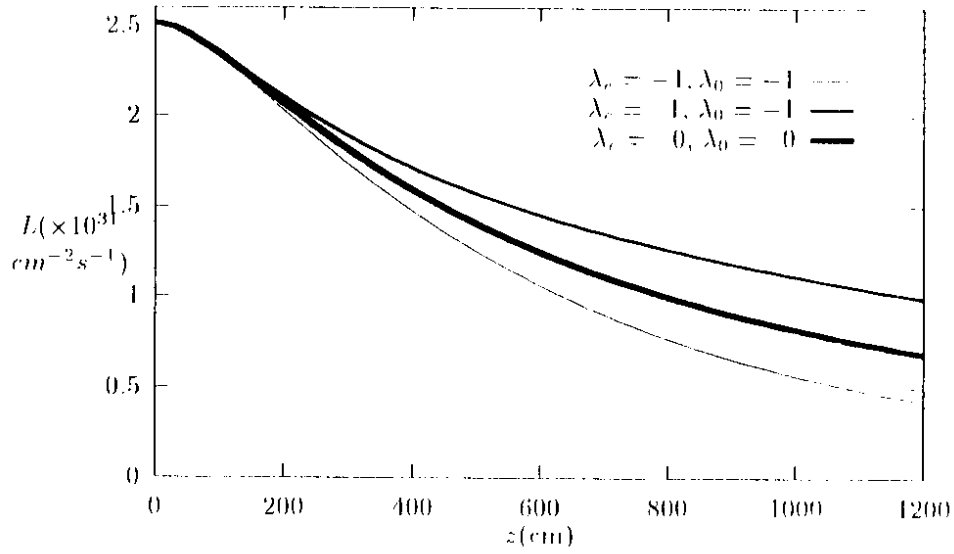

FIG. 3. Dependence of the luminosity on distance between conversion region and collision point(2) for three different choices of polarizations of linac electrons λ_e and laser photons λ_0

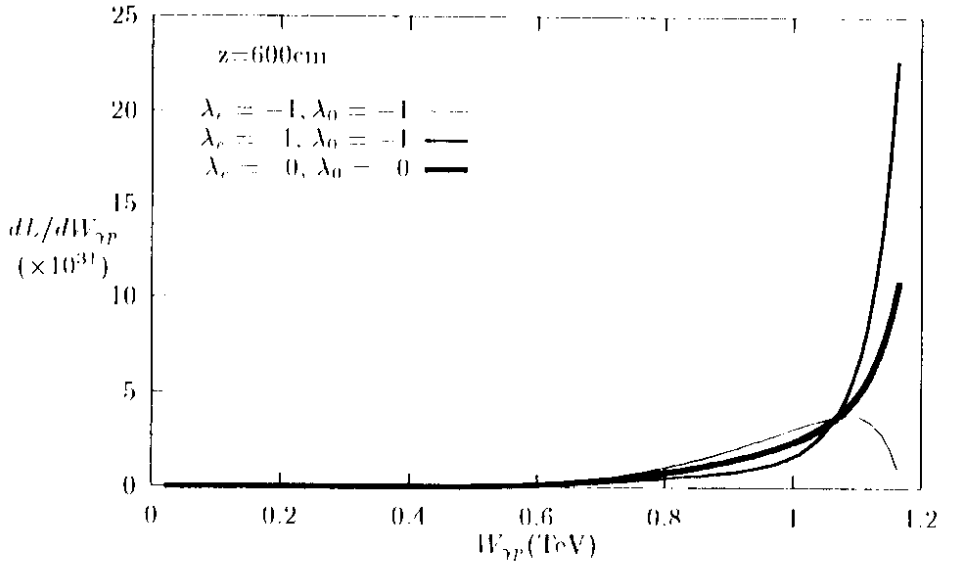

FIG. 4. Luminosity distributions (in units of $cm^{-2}s^{-1}TeV^{-1}$) depending on γp invariant mass at z=6m for three different choices of λ_e and λ_0

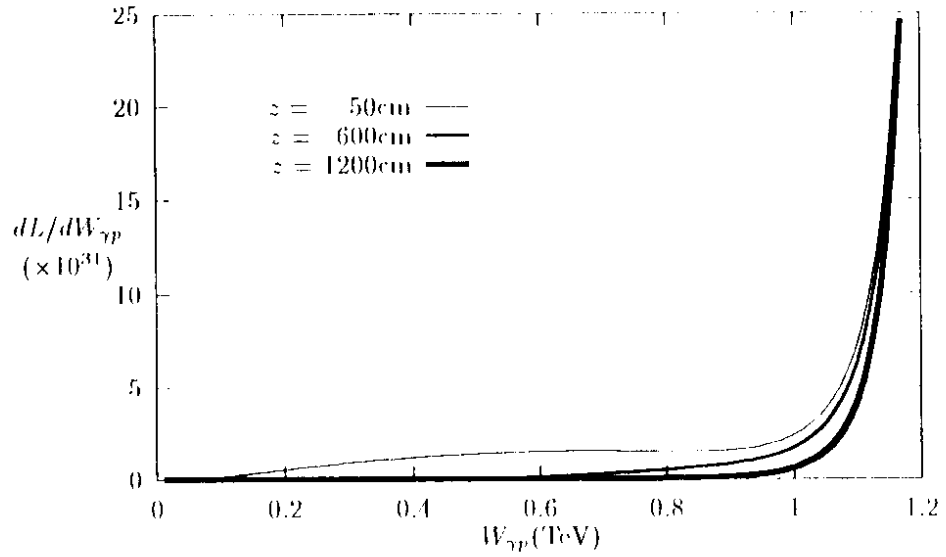

FIG. 5. Luminosity distributions (in units of $cm^{-2}s^{-1}TeV^{-1}$) depending on γp invariant mass for $\lambda_e = 1$ and $\lambda_0 = -1$ choice at three different values of z.

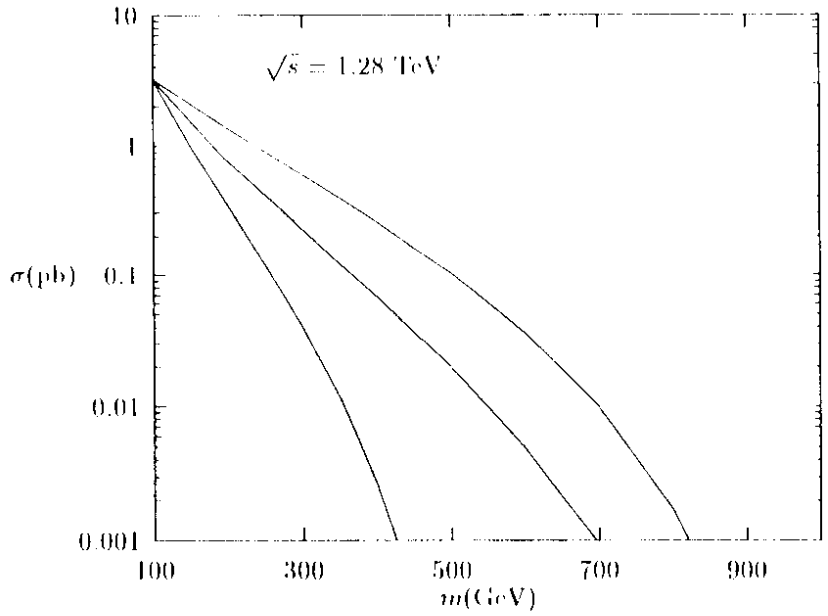

FIG. 6. Production cross sections of chargino and squarks as a function of their masses. The upper curve corresponds to the case $\tilde{m}_u = 100$ GeV, the middle curve to the $\tilde{m}_d = 100$ GeV and the lower curve to the $\tilde{m}_u = \tilde{m}_d$.

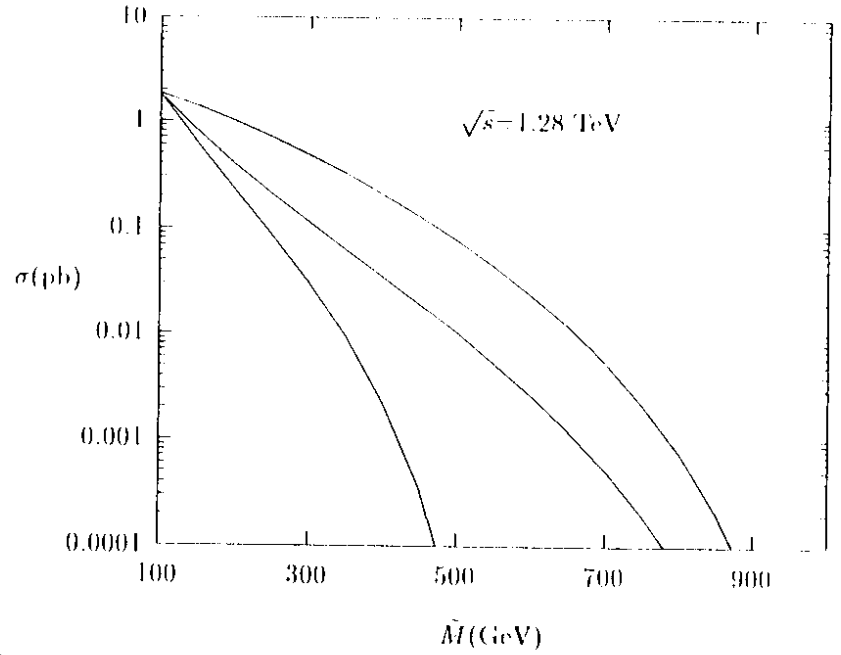

FIG. 7. Production cross section for gluino and squarks as a function of their masses. The upper line corresponds to $\tilde{m}_q = 100$ GeV , the middle line to $\tilde{m}_q = 100$ GeV and the lower line to $\tilde{m}_q = \tilde{m}_g$ cases, respectively.

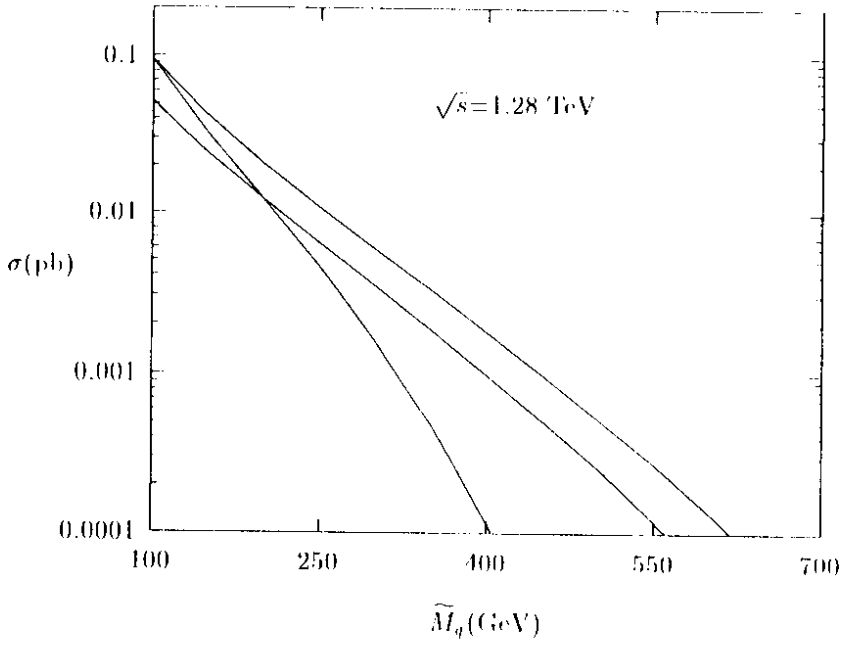

FIG. 8. Production cross section for zino and squarks as a function of squark masses. $\tilde{m}_z = 100$ GeV, $\tilde{m}_z = 200$ GeV and $\tilde{m}_z = \tilde{m}_q$ cases correspond to upper, middle and lower curves, respectively.

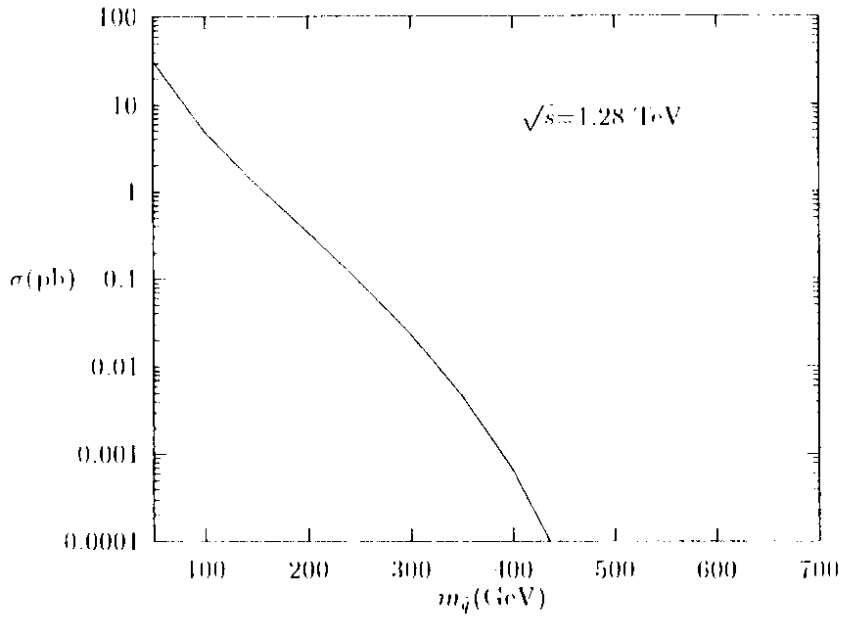

FIG. 9. Production cross sections of squark pairs as a function of their masses

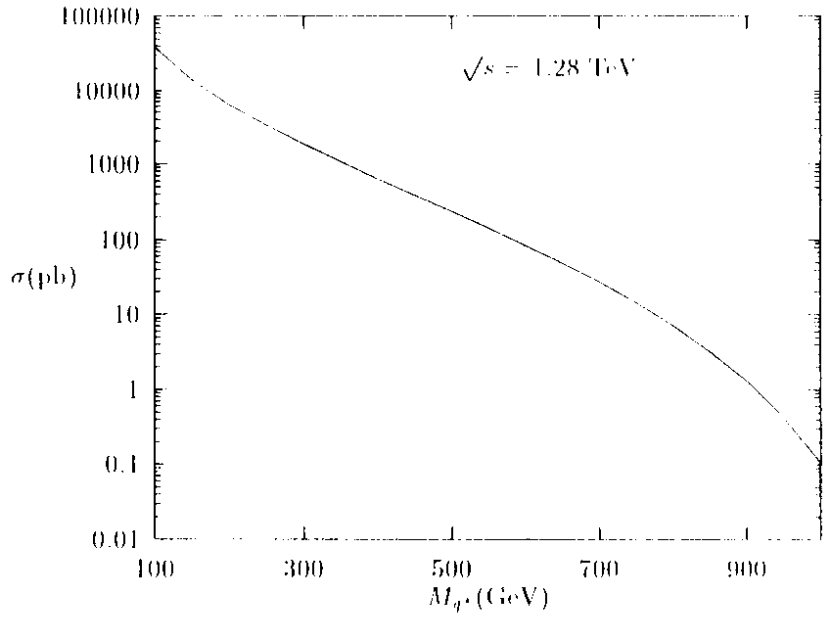

FIG. 10. Total cross sections for the production of excited quark as a function of its mass.

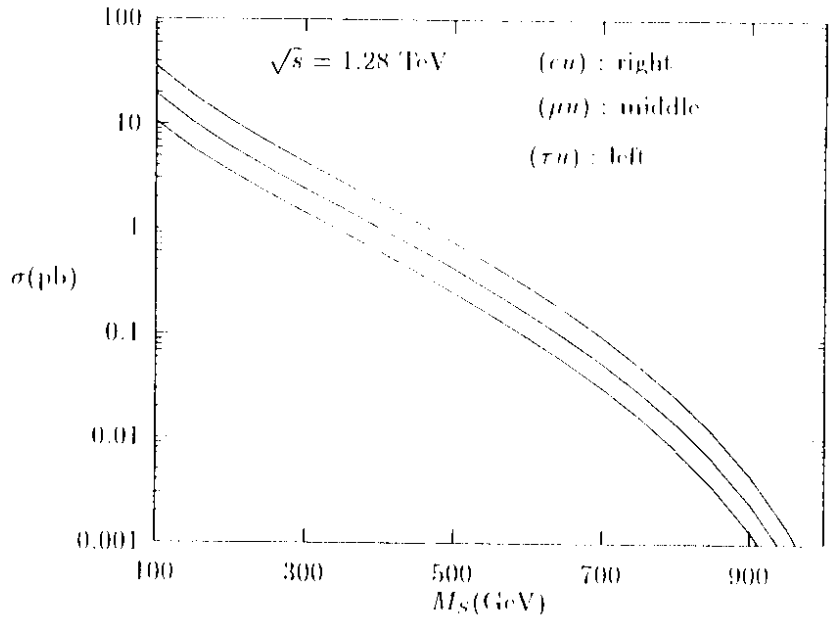

FIG. 11. Total cross sections for single production of scalar leptoquark as a function of its mass.

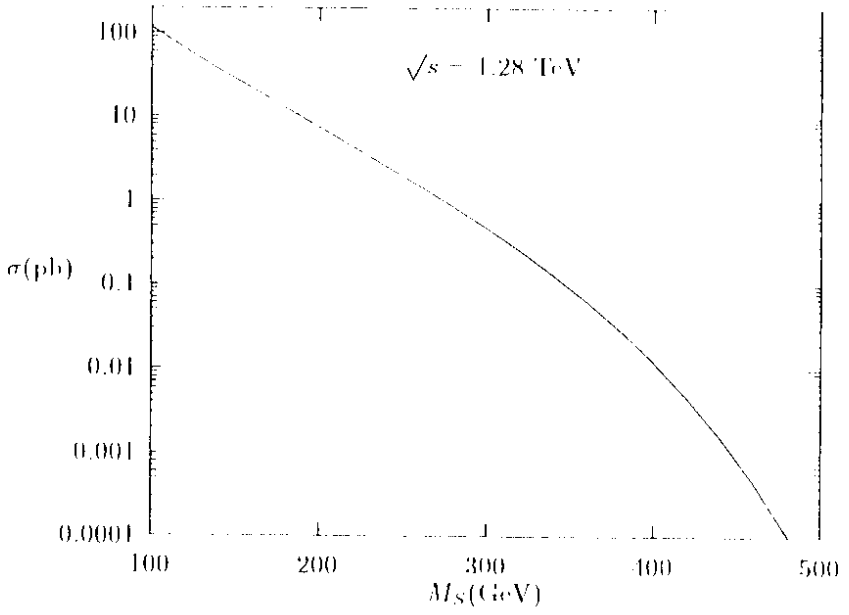

FIG. 12. Total cross sections for pair production of scalar leptoquarks as a function of their masses.

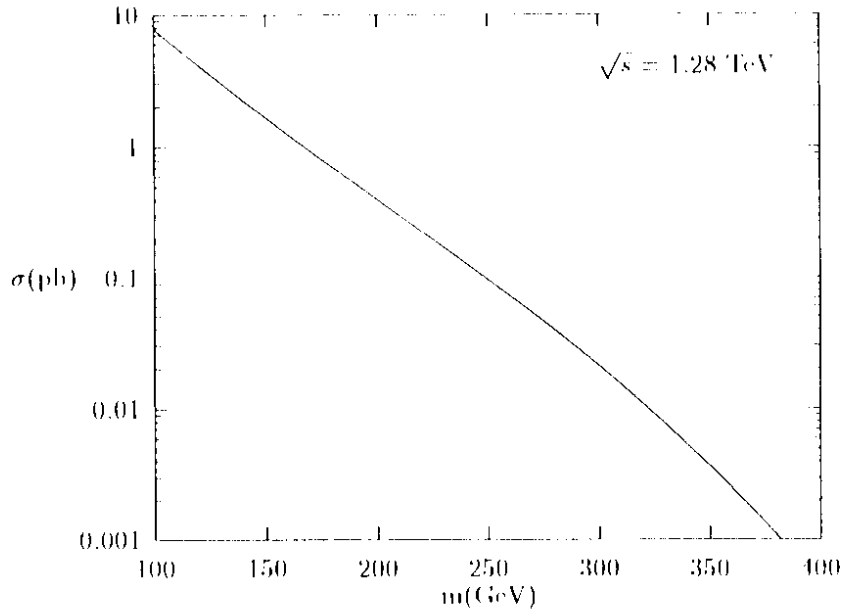

FIG. 13. Total cross section for pair production of Q=2/3 quarks as a function of their masses.

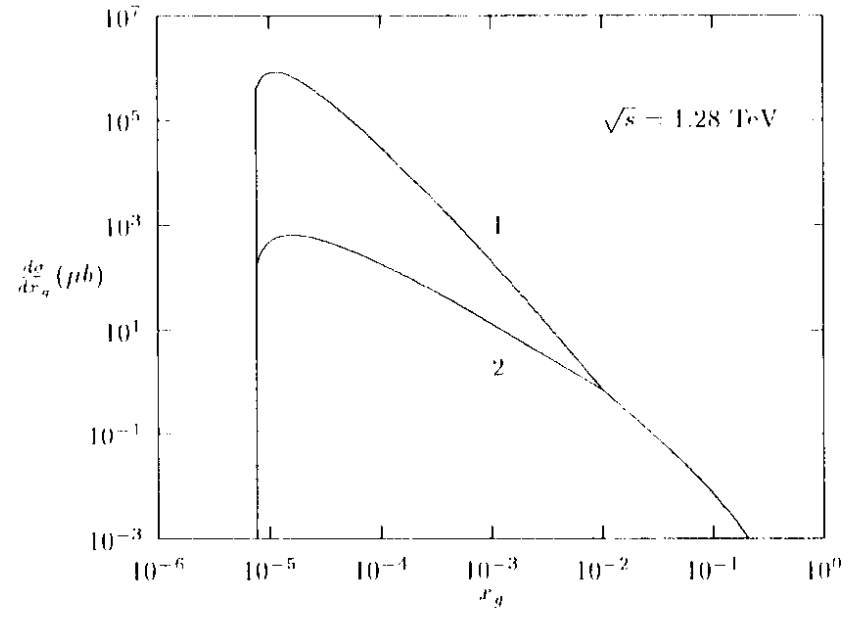

FIG. 14. $d\sigma/dx_g$ for the process $\gamma p \to c\bar{c}X$. Curves 1 and 2 correspond to different parametrizations of gluon distributions.

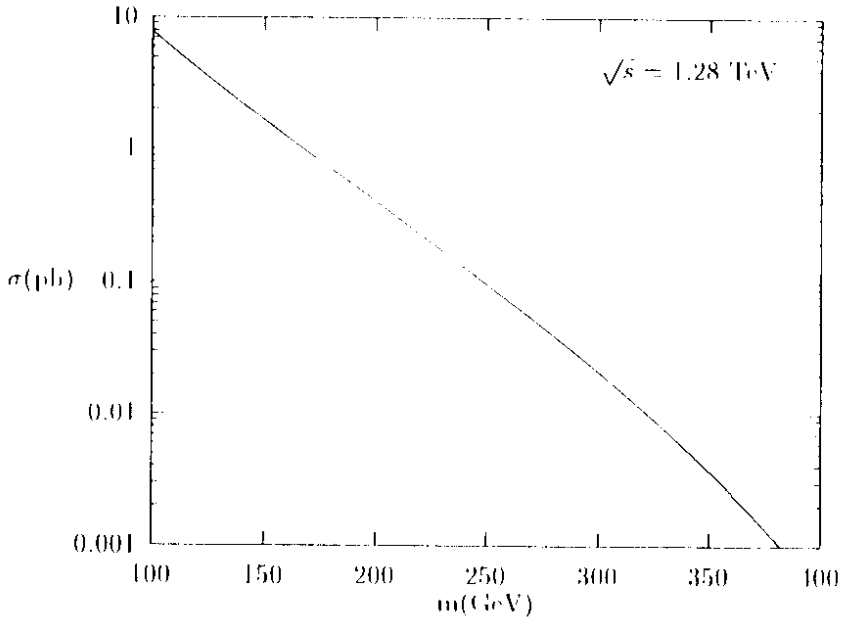

FIG. 13. Total cross section for pair production of Q=2/3 quarks as a function of their masses.

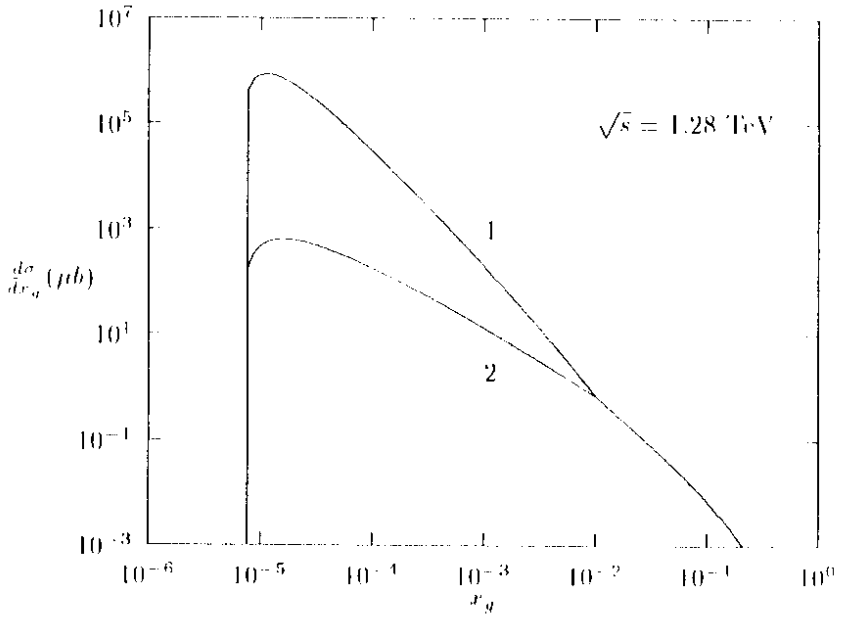

FIG. 14. $d\sigma/dx_g$ for the process $\gamma p \to c\bar{c}X$. Curves 1 and 2 correspond to different parametrizations of gluon distributions.